An Efficient Algorithm for Peak Detection on B-Scan data generated using GPR

Rajath Kumar M.P [1], Nishanth N Bhonsle [2], Smitha N, S.N. Sridhara, Vipula Singh
Department of Electronics and Communication Engineering, R. N. Shetty Institute of Technology (RNSIT), Bangalore, India
[1] rajathkumar.exe@gmail.com
[2] nishanthnbhonsle@gmail.com

***Abstract*— B-Scan data generated using the Ground Penetrating Radar contains information about the apparent location of the landmines and other similar objects buried underground. The peak of the hyperbola so generated in the B-Scan represents the apparent depth and lateral distance of the landmines from the point of operation and these apparent peaks need to be migrated to their true positions using migration technique. Peak-detection is the pre-requisite to determine the apparent location of landmines or any other object buried underground and in this paper we propose an effective and efficient algorithm for the same. The proposed algorithm works for all possible conditions in a specified range given that the landmines are separated by a lateral distance of 21cm which corresponds to a gap of 9-pixels in the B-scan data. Many problems faced by the previously proposed algorithms have been overcome significantly. The point at which the landmine is present is the apex/peak of the hyperbola in the B-scan. In order to eliminate the points of non-interest, the algorithm employs filters and morphological transforms and the nearest neighbor method. Segmentation process is applied to obtain the exact apparent peaks from the transformed image of the B-scan which makes it more capable and efficient.**

Keywords*— *Ground Penetrating Radar, B-scan, Peak Detection, Pre-Processing, Hyperbola, Curve Tracing, Transforms, Nearest Neighbor, Segmentation, Fresnel Kirchhoff.

I. INTRODUCTION

Ground Penetrating Radars used to image the subsurface of the ground involves using the electromagnetic radiation in the microwave band of the radio spectrum, and detecting the reflected signals from the subsurface structures. It is an efficient tool that has many different applications like to detect the presence of landmines. It emits electromagnetic (EM) radio waves into the soil through a wideband antenna and collects the reflected signals. The principle of GPR is almost the same as in seismic wave measurement system except for the carrier signal. The commonly used frequency band of GPR ranges from 100 MHz to 4 GHz. Reflection of the wave is due to the subsurface materials having different dielectric properties. When the properties of one material are different than that of another above it, a reflected wave will be produced. The conductivity level for each material would be different, which produces a certain velocity for the traveling EM waves. Using the reflections and the two-way elapsed time of the EM pulse's travel, a cross-sectional reflection profile is created. A rough surface reflects the incident wave in a diffused manner while a smooth surface tends to reflect the wave in one direction, where the angle between the surface (normal) and the reflected wave is the same as the angle between the surface (normal) and the incident wave. The electrical property of the medium determines the amount of reflection and absorption of the EM wave and subsequently affects the direction and intensity of reflection. A single waveform [say b(x, y, t)] recorded by a GPR, with the antennas at a given position (x,y) is referred to as an A Scan. When moving the GPR antennas on a line along the x-axis, a set of A scans can be gathered, which form a 2-D data set known as a B Scan. The penetration depth of the wave into soil usually depends on two factors: The humidity in the soil and the wavelength of the EM wave. Main objective of this paper is to trace and locate the apparent peaks of the underground landmines, which are approximately located within the depth of 30-40cm for further implementation of the Fresnel-Kirchhoff migration algorithm [6]. Existing curve tracing techniques implement the mean and median follower algorithms for a given data and also in the presence of clutter [1]. In this paper we propose an algorithm that surpasses all the problems and drawbacks encountered in the currently available logics for extracting the peak of a received signal irrespective of the position and interferences if any in case of multiple targets and thus pre-processing it for migration.

II. RELATED WORK

There are ample number of curve related and peak extraction problems which are fundamentally different[2] and in this paper we try to resolve the tracing and apparent peak detection phenomenon under all circumstances and process the data as per the pre-requisite of the Fresnel-Kirchhoff migration algorithm. There are different migration techniques like the phase shift migration approach: background removal, spreading and exponential correction techniques are employed for subsurface and inhomogeneous imaging using synthetic aperture radar [3]. This paper employs an adaptive wiener filter technique to expunge the noise and thus meeting the basic requirement of de-noising [4]. Analogous to this the Non Uniform Fast Fourier Transform, NUFFT algorithm is considered to bypass the problem of non-linear relationship between the uniform frequency samples and the wavenumbers [5]. There are other reconstruction techniques specifically for landmine detection. Stolt migration, microwave tomographic inversion (MWT) and back projection (BP) and the efficiency of such approaches are evaluated using the ROC curves [7]. In this paper, a different transformation algorithm which involves pre-processing of the obtained B-

978-1-4673-6680-9/16/$31.00 ©2016 IEEE

scan is implemented and the peaks of interest for the Fresnel-Kirchhoff algorithm are being detected and segmented. A single-pixel and averaged energy based detection is carried out using the mean and co-variance technique and further enhancement using different transformation and algorithms.

III. PROPOSED BLOCK DIAGRAM

An algorithm is proposed using which the apparent positions of the landmines buried in a specific range can be detected and further given as an input for migration techniques, to determine its true position. The block diagram shown in fig 1 enumerates the different blocks of operation in the peak detection under all possible conditions of the targets. Noise reduction, elimination of intersected points and finding the maximum pixel for each individual target are of much primacy. The positions of such pixels are further calculated depending on the range and resolution of operation.

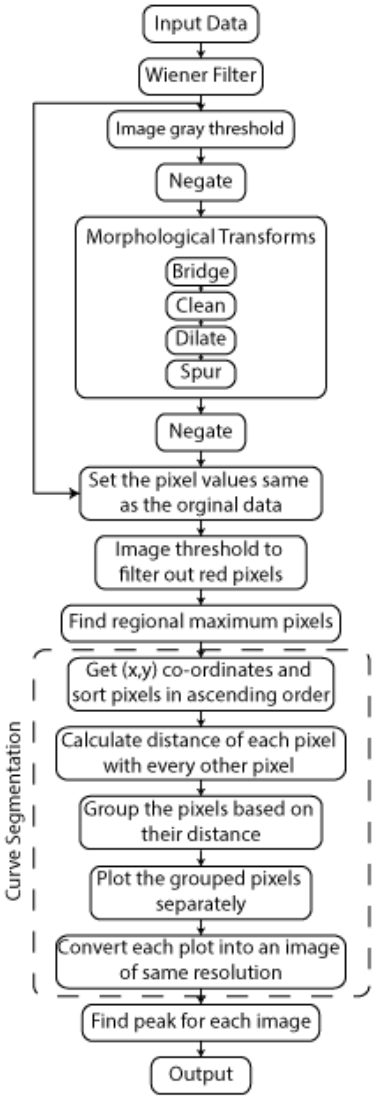

Fig 1. Proposed Block Diagram

IV. ALGORITHM

A. *Generation of input data*

The input B-Scan is simulated by using a stepped frequency waveform of bandwidth 3GHz and divided into 256 equal steps. The back scattered electric field at each spatial point when the frequency is varied from 200MHz to 3.06GHz is stored for all single and multiple target in the range of 200cms in depth. The relative permittivity of the homogeneous ground is chosen to be 9 and the back scattered electric field collected ranges from x=0 to x=6m showing 256 points on range. The results are indicated with respect to pixel co-ordinates by zero centering the origin of the x-axis as shown in fig 2. The cross range is from 0 to 2m and is also divided into 256 points. The B-scan GPR image in the spatial domain is generated by taking the 1-D FFT of the obtained back scattered signal data in the frequency domain and this image exhibits the hyperbolic defocusing behavior.

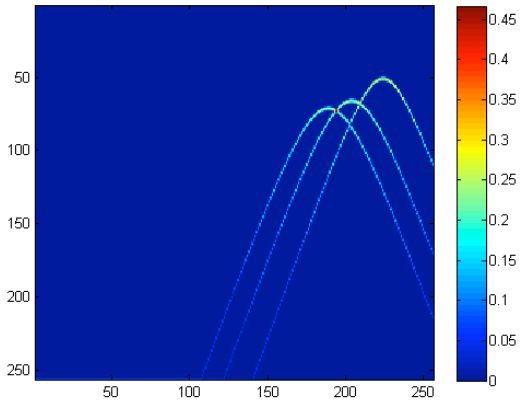

Fig 2. Generated B-scan Data

B. *Wiener Filter*

The filter can be considered as an optimal adaptive filter used as a fundamental approach for noise reduction and can be delineated in different forms for various applications. It is an effective tool for noise suppression without causing any significant detrimental effects to the image in terms of quality and originality [8]. It low-pass filters a gray-scale image that has been deteriorated by constant power additive noise. It adopts a pixel-wise adaptive algorithm based on the statistics (mean and variance from a local neighborhood of each pixel). By default, it would be 3-by-3 neighborhood and the corresponding mean and standard deviation will be estimated. Using this filter, the additive noise before filtering can also be retrieved. Local mean and variance estimation around each pixel:

$$\mu = \frac{1}{NM} \sum_{n_1 n_2 \in n} a(n_1, n_2)$$

$$\sigma^2 = \frac{1}{NM} \sum_{n_1 n_2 \in n} a^2(n_1, n_2) - \mu^2$$

Where,

μ = mean of all the pixels in the image

σ = variance of all the pixels in the image

n = N-by-M local neighborhood of each pixel in the image

The pixel-wise filter estimation:

$$b(n_1,n_2) = \mu + \frac{\sigma^2 - v^2}{\sigma^2}(a(n_1,n_2) - \mu)$$

Where,

v^2 is the noise variance. If noise variance is unknown then the filter uses the average of the local estimated variances. By comparing fig2 and fig3 it is evident that the wiener filter suppresses the points of non-interest.

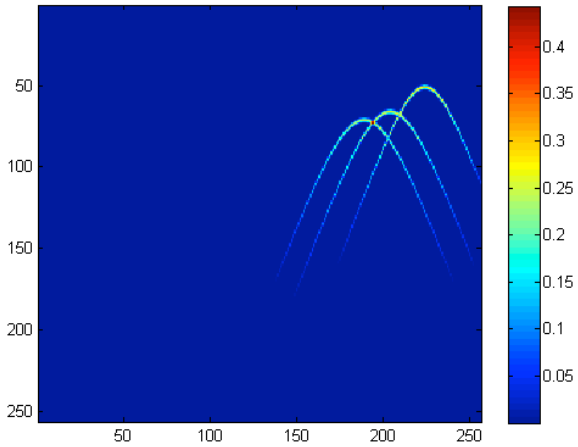

Fig 3. Wiener Filter Result

C. *Gray Thresholding*

The gray-scale image is converted into a binary image by replacing all the pixels in the input image with luminance in the range of threshold (0.06 to 0.35) with a value 1. The remaining pixels are replaced with a value 0. The pixel value 1 corresponds to white and the latter corresponds to black.

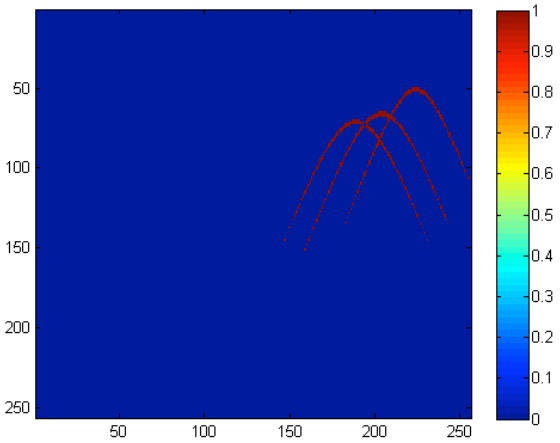

Fig 4. Gray Threshold Result

Note that the intersection of hyperbolas will yield a maximum pixel value which is true even for the peak of the hyperbola. Thus if the intersection is not eliminated then false peaks will be shown at the intersecting points.

D. *Negate*

All pixel values are replaced with the new values obtained by complementing the image by subtracting each pixel value from the maximum pixel value in the original image. This is done to apply morphological transforms.

E. *Morphological Transforms*

Morphological transforms are a collection of non-linear operations which involve shape or morphological features in an image. It depends on relative ordering of pixel values and not on the numerical values. As eradication of pixels of non-interest is of priority, the following morphological transforms are used.

- Bridge transform - The unconnected pixels in the wiener filtered image are connected by toggling the 0-valued pixels to 1, in-case there are two non-zero pixels that are not connected in its neighborhood.
  Depiction:

1 0 0		1 1 0
1 0 1	becomes	1 1 1
0 0 1		0 1 1

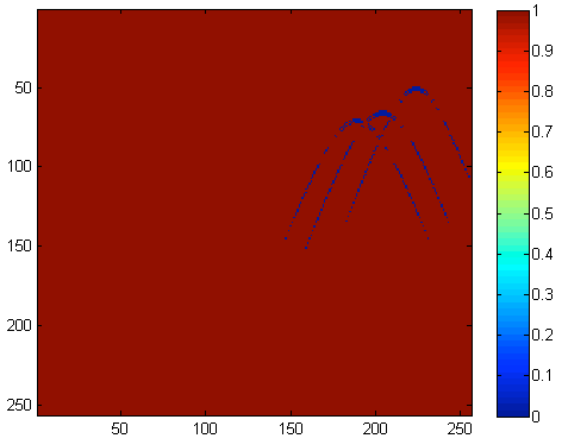

Fig 5. Bridge Transform Result

- Clean transform - The isolated pixels are removed by inspecting its neighborhood and if no non-zero pixel is found then the pixel value would be made 0 and thereby eradicating such pixels which are residues of noise.
  Depiction:

0 0 0		0 0 0
0 1 0	becomes	0 0 0
0 0 0		0 0 0

- Dilate transform - The boundaries of the curves are enhanced by adding pixels at the boundaries and making them 1, even if one of the pixels in the neighborhood defined by the structuring element is 1 :

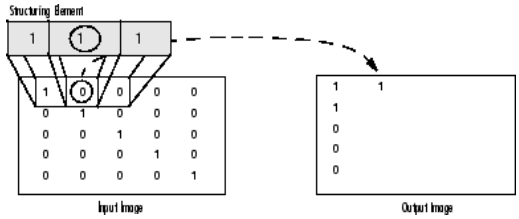

Fig 6. Dilate Transform

- Spur algorithm - The pixels that have exactly one 8-connected neighborhood are removed and thereby enhancing the image for peak extraction by removing the endpoints of the curve.
  Depiction:

0 0 0 0		0 0 0 0
0 0 0 0		0 0 0 0
0 0 1 0	becomes	0 0 0 0
0 1 0 0		0 1 0 0
1 1 0 0		1 1 0 0

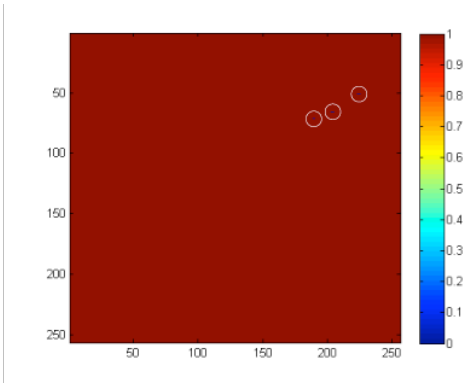

Fig 7. Spur Transform Result

F. *Negate and Threshold*

Negating the image again will restore the original pixel values and thereby restoring the original image with only pixels of interest thus enabling it for further thresholding. Thresholding of pixel values in the range of 0.19 to 0.35 will yield the peaks as these pixel values correspond to the shades of red. This is because the peak of the hyperbola generated from the B scan will have the maximum pixel value.

G. *Regional Maximum*

As discussed above, the peak will have the highest pixel value, hence by filtering out the maxima in the image which will have the same pixel intensity even in it's neighborhood we will be able to filter out only the pixels which corresponds to the peak.

H. *Curve Segmentation*

The image subjected to regional maximum would contain only the maximum pixel values. The maximum pixel location value of the image returns only the position of the highest peak but fails to output the location of the other two peaks. To overcome this problem curve segmentation is implemented. The entire image is translated into discrete forms and the nearest neighbor method is applied. The pixels which are close to each other are grouped and these grouped pixels are then plotted distinctly, thus separating the curves from one another. Now for each image, applying the maximum function would return the location of the peaks and this is exemplified in the results section.

V. RESULTS

The different possible scenarios of the land-mines buried underground in real world conditions are used as test cases for the algorithm. For each scenario, the results are tabulated which depict the peak pixel values returned by the algorithm of the multiple targets individually and also the correspondingly calculated lateral distance and depth of the landmines respectively. The different possibilities are that the landmines can be placed at the same cross range but different lateral positions as shown in fig 8. They might be placed with very less lateral distance and cross range as shown in fig 10 where the detection of the peaks is complex. In such cases, the nearest neighbor method is implemented for high accuracy in finding the peaks. Other possible scenarios are when the landmines are placed at the same lateral position and varying their cross ranges as shown in fig 12. In some cases, the hyperbola of any target would partially be out of the range of operation as shown in fig 14. There might be a scenario as shown in fig 16 where the target peaks of the targets coincide with the intersection points of the hyperbolas and peak detection would be very intricate. The peak pixel value corresponding to the lateral distance would be greater by 128 pixels due to the zero centering and hence the obtained value must be subtracted by 128 in each case. The obtained apparent peak pixel values would be incremented by a value of 1 due to the image indexing starting from 1 and hence the obtained pixel values must be decremented by 1 for accurate results. The lateral distance and depth of a landmine is computed from the determined pixel values of the peak of the corresponding hyperbola (say peak is [x, y]), from the following relation that if a lateral distance of 6 meters corresponds to 256 pixels then x pixels would correspond to what lateral distance and similarly if a depth of 2 meters corresponds to 256 pixels then y pixels would correspond to what depth in meters. The algorithm works for all cases irrespective of the cross ranges of the targets but the only caveat is that there must be a 9-pixel gap in their lateral positions that is equivalent to 21cm lateral distance between the landmines under consideration as shown in fig 18 which is very unlikely in real world conditions.

A. *Case 1*

The targets in the B-scan as shown in fig 8 are at the same cross range (depth) and vary in their lateral distances and hence engendering intersected points which appear to be the peaks. The algorithm eliminates such points of

intersection and detects only the peaks of interest. The apparent depth and lateral position of each peak is enumerated by considering the lateral and cross ranges for their corresponding pixel values and the results are tabulated in table 1.

B. Case 2

The peak of the target that is placed deeper than the other two targets as shown in fig 10 coincides with the point of intersection and thus thresholding in such cases leads to loss of relevant data. In such scenarios, the algorithm extracts multiple points instead of one point for each target. The nearest neighbor algorithm is implemented to segment each curve and to obtain the regional peak value for each target and the results are tabulated in table 2.

C. Case 3

The targets are placed in such a way that they all have the same lateral position but vary in their cross ranges (depth) as shown in fig 12. The detection of the peaks by the algorithm would be easy in such cases as the tip of the hyperbolas would not involve in any intersections and can be easily done by merely thresholding the B-scan as mentioned previously. The results are tabulated in table 3.

D. Case 4

One of the hyperbolas in the B-scan of the targets of interest escapes from the range of operation and in such scenarios, the detection of the target depends completely upon the position of the peak of such hyperbola as shown in fig 14. Until and unless the peak is lost from the range, irrespective of the portion of the hyperbola present in the B-scan, the exact position of such peaks can be detected using the algorithm and the results are tabulated in table 4.

E. Case 5

The peaks of interest of the targets under consideration coincide with the intersection points and this poses a problem as there is a possibility that the algorithm might eliminate such peaks as shown in fig 16. But under such scenario, the nearest neighborhood logic is implemented by the algorithm to give a series of points for each target location. The peak of such series can be detected by using the regional maximum logic and thus getting a single pixel of interest and the results are tabulated in table 5.

F. Case 6

It is evident from fig 19, that the third peak is lost while detection of the targets in fig 18. Such loss occurs when the regional max operation of the images is carried out. When any two peaks are in the same neighborhood then the pixel with higher intensity suppresses the peak pixel with lower intensity thus leading to loss of pixels. Similarly the losses may occur when the nearest neighbor algorithm is applied to the transformed image when the distance between the peaks is less than 21cm which corresponds to 9 pixels in the B-scan data. When the algorithm is applied, the nearby peaks are grouped and segmented as a single image hence only the higher peak is located. Thus the algorithm fails to distinguish between the peaks under consideration and the results are tabulated in table 6.

VI. CONCLUSION

The proposed algorithm succeeds in finding the apparent peaks from the B-Scan data with accuracy of 100 percent but fails for conditions as discussed in case 6. Eliminating the pixels of non-interest, by the method of thresholding at each operation increases the probability of finding the apparent peaks. Nearest neighbor method and segmentation of each hyperbola simplify the process of finding the peaks without any compromise on accuracy which would otherwise be byzantine in a few cases. The algorithm clocks on an average of 0.7794 seconds of run time. The results obtained as the apparent peaks were given as input to Fresnel Kirchhoff migration technique which enabled migration to their true positions. Thus, the paper discusses an efficient and accurate algorithm to meet the pre-requisite of the migration process in the detection of landmines and other similar applications.

VII. ACKNOWLEDGEMENT

The algorithm was developed in GPR Lab, Dept. of ECE, RNSIT under the guidance of Asst. Prof Smitha N, Prof S.N. Sridhara and Dr. Vipula Singh. This work has been carried out under AICTE Grant No. 20/AICTE/RFID/RPS (POLICY IV) 2012-2013, we are thankful to AICTE for supporting this project.

VIII. REFERENCES

[1] A curve tracing algorithm using level set based affine transforms Lam, B.S.Y.; Van, H. Systems, Man and Cybernetics, 2005 IEEE International Conference on Year: 2005, Volume: 3

[2] Improved curve tracing in images Raghupathy, K.; Parks, T.W. Acoustics, Speech, and Signal Processing, 2004. Proceedings. (ICASSP '04). IEEE International Conference on Year: 2004, Volume: 3.

[3] Radar subsurface imaging by phase shift migration algorithm Hui Zhang; Benedix, W.-S.; Plettemeier, D.; Ciarletti, V.Radar Conference (EuRAD), 2013 European Year: 2013

[4] Iterative Edge-Preserving Adaptive Wiener Filter for Image Denoising. Chikako Abe and Tetsuya Shimamura. International Journal of Computer and Electrical Engineering, Vol. 4, No. 4, August 2012

[5] Two-dimensional and three-dimensional NUFFT migration method for landmine detection using ground-penetrating Radar Jiayu Song; Qing Huo Liu; Torrione, P.; Collins, L. Geoscience and Remote Sensing, IEEE Transactions on Year: 2006, Volume: 44, Issue: 6

[6] FFT implementation of Kirchhoff's migration for ground penetrating radar image focussing Sharma, S.; Thangarasu, P.; Jena, P.; Kuloor, R. Computer Communication and Informatics (ICCCI), 2012 International Conference on Year: 2012

[7] A Comparative Study of GPR Reconstruction Approaches for Landmine Detection Gonzalez-Huici, M.A.; Catapano, I.; Soldovieri, F. Selected Topics in Applied Earth Observations and Remote Sensing, IEEE Journal of Year: 2014, Volume: 7, Issue: 12

[8] New Insights Into the Noise Reduction Wiener Filter Jingdong Chen, Jacob Benesty, Yiteng (Arden) Huang, and Simon Doclo IEEE transactions on audio, speech, and language processing, vol. 14, no. 4, july 2006

[9] Adaptive wiener filtering of noisy images and image sequences F. Jin, P. Fieguth, L. Winger and E. Jernigan Department of Systems Design

Engineering University of Waterloo Waterloo, Ontario, Canada, N2L 3G1

[10] J. S. Lee, "Digital image enhancement and noise filtering by use of local statistics,," *IEEE Trans. PAMI*, vol. 2, pp. 165–168, 1980.

[11] S. G. Chang, B. Yu, and M. Vetterli, "Image denoising via lossy compression and wavelet thresholding," *IEEE Trans. IP*, vol. 9, pp. 1532–46, 2000.

[12] J. C. Brailean, R. P. Kleihorst, S. Efstratiadis, A. K. Katsaggelos, and R. L. Lagendijk, "Noise reduction filters for dynamic image sequences, a review," *Proc. IEEE*, vol. 83, pp. 1272–92, 1995.

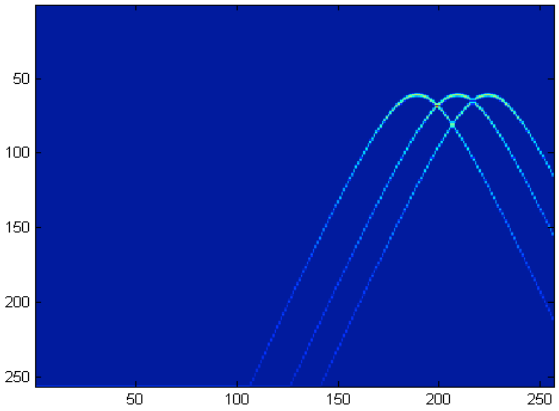

Fig 8. Input Data for Case 1

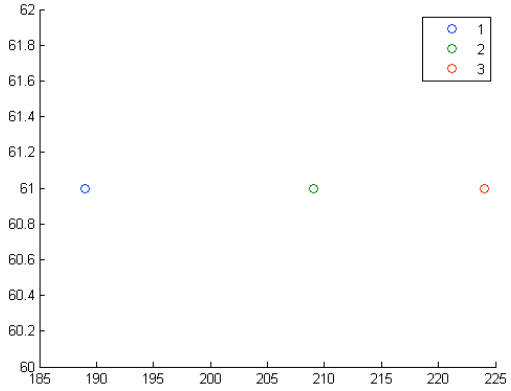

Fig 9. Result of Case 1

Table 1

INPUT VALUES		OUTPUT VALUES		ERROR [L,D] (CM)
PIXEL VALUE	LATERAL DISTANCE (L) DEPTH(D) (CM)	PIXEL VALUE	LATERAL DISTANCE (L) DEPTH(D) (CM)	
(60,60)	(140.62,46.87)	(188,60)	(140.62,46.87)	[0,0]
(80,60)	(187.5,46.87)	(208,60)	(187.5,46.87)	[0,0]
(95,60)	(222.65,46.87)	(223,60)	(222.65,46.87)	[0,0]

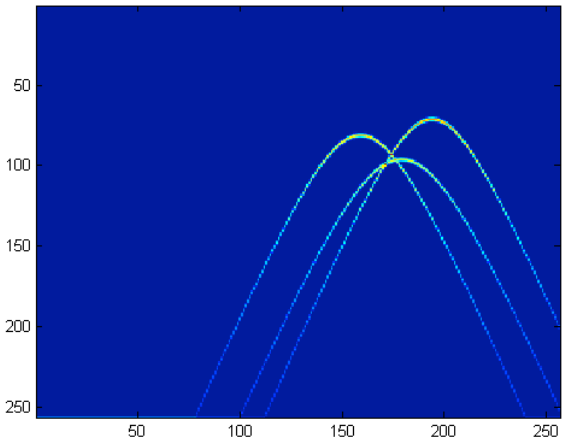

Fig 10. Input Data for Case 2

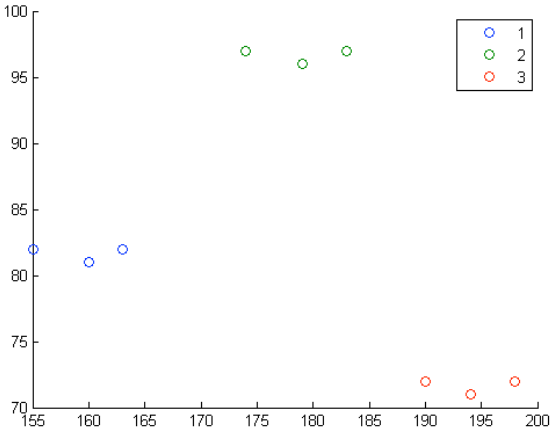

Fig 11. Result of Case 2

Table 2

INPUT VALUES		OUTPUT VALUES		ERROR [L,D] (CM)
PIXEL VALUE	LATERAL DISTANCE (L) DEPTH(D) (CM)	PIXEL VALUE	LATERAL DISTANCE (L) DEPTH(D) (CM)	
(30,80)	(70.31,62.5)	(158,80)	(70.31,62.5)	[0,0]
(50,95)	(117.18,74.21)	(178,95)	(117.18,74.21)	[0,0]
(65,70)	(152.34,54.68)	(193,70)	(152.34,54.68)	[0,0]

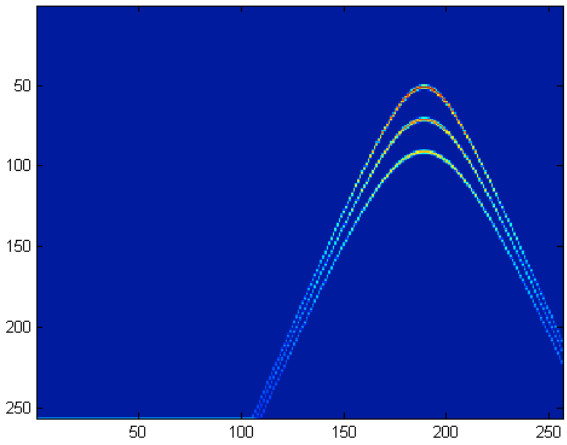

Fig 12. Input Data for Case 3

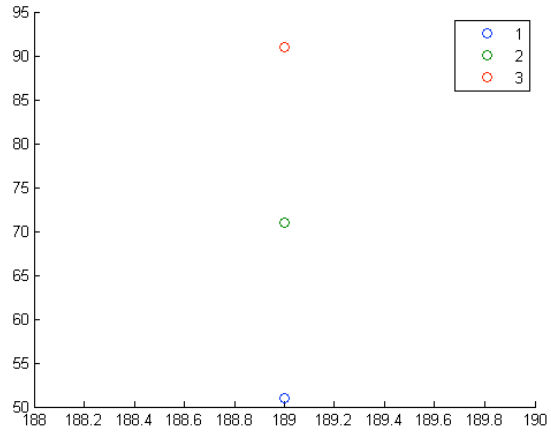

Fig 13. Result of Case 3

Table 3

INPUT VALUES		OUTPUT VALUES		ERROR [L,D] (CM)
PIXEL VALUE	LATERAL DISTANCE (L) DEPTH(D) (CM)	PIXEL VALUE	LATERAL DISTANCE (L) DEPTH(D) (CM)	
(60,70)	(140.62,54.68)	(188,60)	(140.62,54.68)	[0,0]
(60,50)	(140.62,39.06)	(188,50)	(140.62,39.06)	[0,0]
(60,90)	(140.62,70.31)	(188,90)	(140.62,70.31)	[0,0]

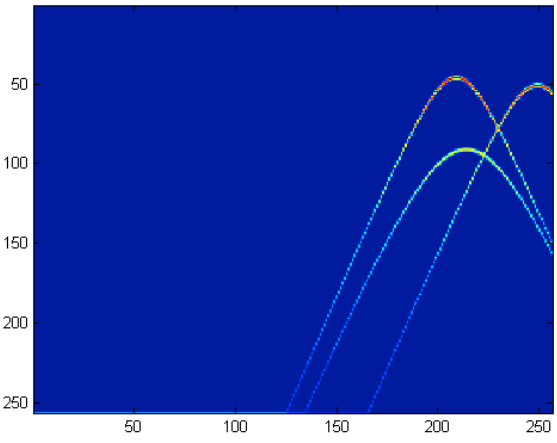

Fig 14. Input Data for Case 4

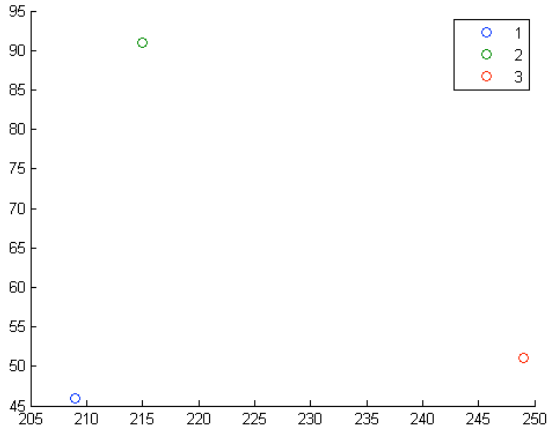

Fig 15. Result of Case 4

Table 4

INPUT VALUES		OUTPUT VALUES		ERROR [L,D] (CM)
PIXEL VALUE	LATERAL DISTANCE (L) DEPTH(D) (CM)	PIXEL VALUE	LATERAL DISTANCE (L) DEPTH(D) (CM)	
(80,45)	(187.5,35.15)	(208,45)	(187.5,35.15)	[0,0]
(120,50)	(281.25,39.06)	(248,50)	(281.25,39.06)	[0,0]
(85,90)	(199.21,70.31)	(213,90)	(199.21,70.31)	[0,0]

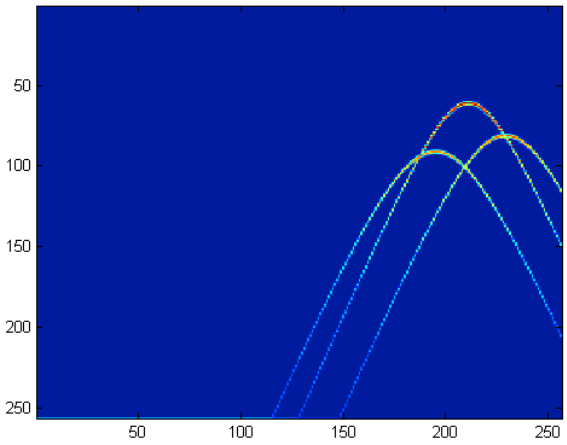

Fig 16. Input Data for Case 5

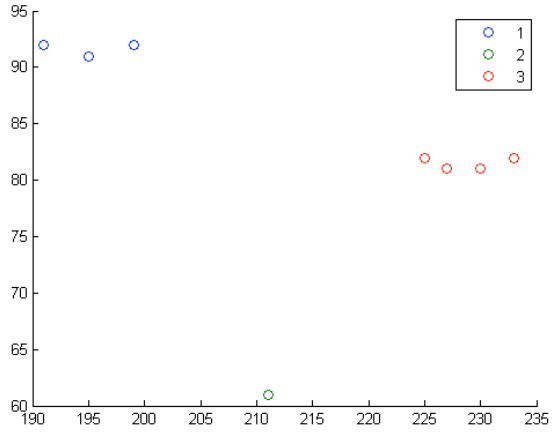

Fig 17. Result of Case 5

Table 5

INPUT VALUES		OUTPUT VALUES		ERROR [L,D] (CM)
PIXEL VALUE	LATERAL DISTANCE (L) DEPTH(D) (CM)	PIXEL VALUE	LATERAL DISTANCE (L) DEPTH(D) (CM)	
(100,80)	(234.34,62.5)	(228,80)	(234.34,62.5)	[0,0]
(66,90)	(154.68,70.31)	(194,90)	(154.68,70.31)	[0,0]
(82,60)	(192.18,46.87)	(210,60)	(192.18,46.87)	[0,0]

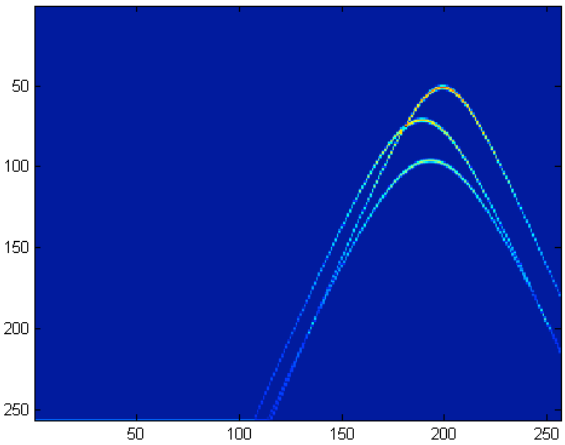

Fig 18. Input Data for Case 6

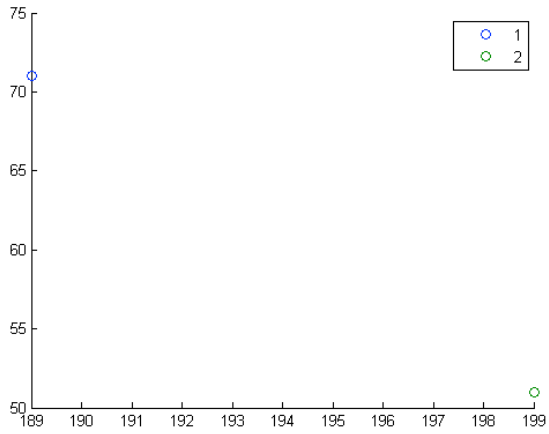

Fig 19. Result of Case 6

Table 6

INPUT VALUES		OUTPUT VALUES		ERROR [L,D] (CM)
PIXEL VALUE	LATERAL DISTANCE (L) DEPTH(D) (CM)	PIXEL VALUE	LATERAL DISTANCE (L) DEPTH(D) (CM)	
(60,70)	(140.62,54.68)	(188,71)	(140.62,54.68)	[0,0]
(70,50)	(164.06,39.06)	(199,51)	(164.06,39.06)	[0,0]
(64,95)	(150,74.21)	PEAK LOST		